Design of Multistate Diplexers on Uniform- and Stepped-Impedance Stub-Loaded Resonators

Zhi-Chong Zhang, Sai-Wai Wong, *Senior Member, IEEE*, Jing-Yu Lin, *Student Member, IEEE*, Haiwen Liu, *Senior Member, IEEE*, Lei Zhu, *Fellow, IEEE*, and Yejun He, *Senior Member, IEEE*

***Abstract*— This paper presents the proposal and design of multistate diplexer on uniform- and stepped stub-loaded resonators, that is, a three-state diplexer (TSD) and a four-state diplexer (FSD). The two proposed diplexers have an attractive application in a frequency-hopping system with miniaturization in their overall size. Next, three and four sets of second-order bandpass filters are applied to form the three and four filtering channels, respectively. These filtering channels are then used to comprise these multiple-state diplexers. In this way, compact size and high-frequency selectivity have been well achieved. For the purpose of demonstration, the prototypes of TSD and FSD are fabricated and measured. The measured results are found in good agreement with the simulated results.**

***Index Terms*— Four-state diplexer (FSD), multistate diplexer, planar circuit, second order, three-state diplexer (TSD).**

I. Introduction

A DIPLEXER is one of the crucial components used for channel selection, signal synthesis, and frequency separation in wireless communication systems. As highly demanded, the design and synthesis of a diplexer has been widely studied. There are several approaches reported in the literature to design a variety of diplexers [1]–[16]. Among them, there are two typical structures: planar structures based on microstrip line [1]–[5], substrate integrated waveguide [6]–[8], coplanar waveguide [9], and slot line [10] and cavity structures based on waveguide cavity [11]–[13], coaxial cavity [14], and dielectric resonator loaded cavity [15], [16]. These diplexers have their own advantages, such as low loss, high isolation, low cost, compact size, high unloaded Q factor, and high power capacity. However, all the aforementioned diplexers can only be applied for the typical uplink and downlink systems. Thus, multiple channel systems require multiple diplexers, which lead to large size and high cost.

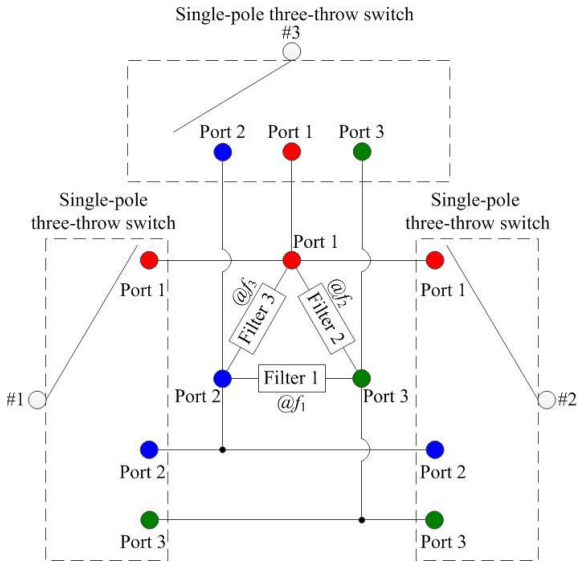

Fig. 1. Schematic of the proposed TSD circuit topology used for frequency-hopping communication.

A three-state diplexer (TSD) is a kind of highly integrated multifunctional diplexer. As shown in Fig. 1, combined with single-pole-three-throw switch circuits, a TSD is applied to achieve a three-port network frequency-hopping circuit with circuit miniaturization. There are three frequency states for a frequency-hopping system to be switched freely. The concept of TSD is first presented in [17]. Then, a planar triple-mode elliptical-shaped resonator is used for achieving this functionality. Herein, two TM_{11} degenerate modes and one TM_{21} mode are used to form three filtering channels, which are further combined to generate three states of TSD. However, only one transmission pole emerges in each passband, so this TSD suffers from poor passband flatness and poor inband selectivity. Moreover, it is difficult to implement more states, thus blocking it from real applications. How to design a planar compact high-order TSD with more than three states under operation has not yet been reported in the literature.

Manuscript received July 30, 2018; revised November 9, 2018; accepted December 13, 2018. Date of publication February 1, 2019; date of current version April 3, 2019. This work was supported in part by the Shenzhen Science and Technology Programs under Grant JCYJ 20170302150411789, Grant JCYJ 20170302142515949, and Grant GCZX 2017040715180580, in part by the National Natural Science Foundation of China under Grant 61861022, in part by the Guangdong Provincial Science and Technology Program under Grant 2016B090918080, in part by the NTUT-SZU Joint Research Program under Grant 2018009, and in part by the Shenzhen University Research Startup Project of New Staff under Grant 20188082. *(Corresponding author: Sai-Wai Wong.)*

Z.-C. Zhang is with the College of Electronic and Information Engineering, Jinggangshan University, Ji'an 343009, China.

S.-W. Wong and Y. He are with the College of Information Engineering, Shenzhen University, Shenzhen 518060, China (e-mail: wongsaiwai@ieee.org).

J.-Y. Lin is with the School of Electrical and Data Engineering, University of Technology Sydney, Ultimo, NSW 2007, Australia.

H. Liu is with the School of Electronic and Information Engineering, Xi'an Jiaotong University, Xi'an 710049, China.

L. Zhu is with the Department of Electrical and Computer Engineering, University of Macau, Macau 999078, China.

Color versions of one or more of the figures in this paper are available online at http://ieeexplore.ieee.org.

Digital Object Identifier 10.1109/TMTT.2019.2893656

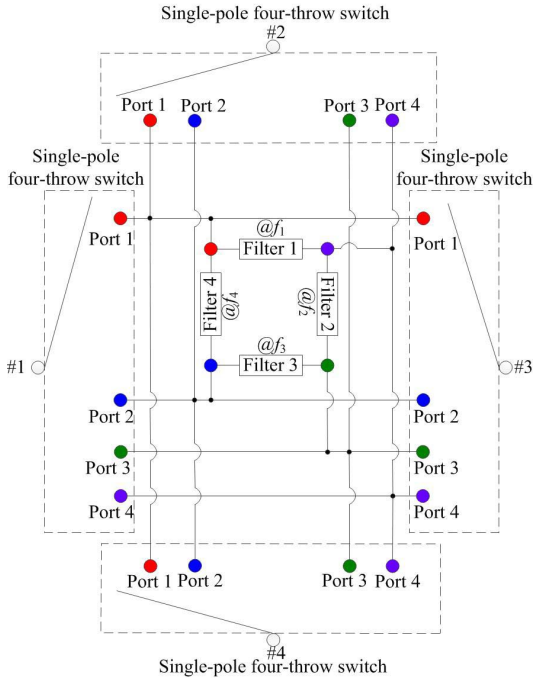

Fig. 2. Schematic of the proposed FSD circuit topology used for frequency-hopping communication.

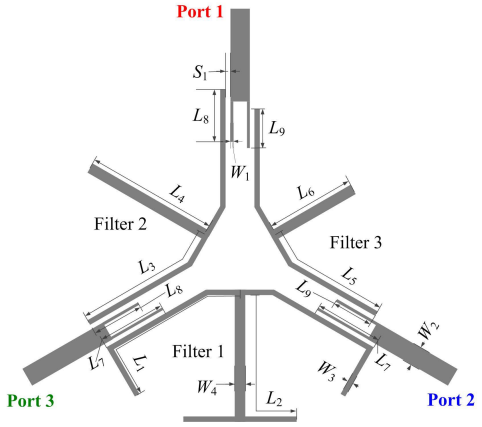

Fig. 3. Configuration of the proposed TSD on the microstrip line structure.

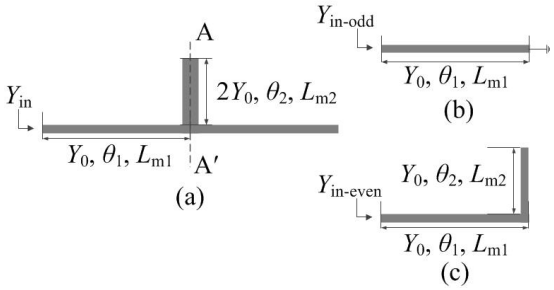

Fig. 4. (a) Layout of SLR. (b) Odd-mode equivalent circuit. (c) Even-mode equivalent circuit.

In this paper, a compact second-order TSD using the uniform-impedance stub-loaded resonator (SLR) is presented at first. Its passband flatness and frequency selectivity are exhibited to get a great improvement. On the basis of the designed TSD, a second-order four-state diplexer (FSD) is then presented with more compactness. As shown in Fig. 2, by combining with single-pole-four-throw switch circuits, the FSD can be employed for developing a four-port network frequency-hopping circuit, where four frequency states for frequency-hopping system can be switched freely.

II. Second-Order TSD Design

A. Configuration

The corresponding configuration of second-order TSD on the microstrip line structure is shown in Fig. 3. It consists of three second-order bandpass filters (BPFs) and three microstrip feed lines. It involves a uniform-stepped SLR in the design of three second-order BPFs [19], [20]. The center frequencies of the three BPFs (Filter 1, Filter 2, and Filter 3) are denoted by f_{TSD1}, f_{TSD2}, and f_{TSD3}, respectively, wherein $f_{\mathrm{TSD1}} < f_{\mathrm{TSD2}} < f_{\mathrm{TSD3}}$. Compared with traditional diplexers, each port of TSD can operate at two frequencies, which makes this TSD holding three operating states as a multifunctional diplexer. In this paper, the printed circuit board with a relative dielectric constant of $\varepsilon_r = 2.55$, a loss tangent $\tan\delta = 0.003$, and a thickness of $h = 0.8$ mm is used to design and fabricate the proposed TSD and FSD.

B. Stub-Loaded Resonator

Fig. 4(a) shows the layout of SLR. The equivalent circuits of odd mode and even mode are depicted in Fig. 4(b) and (c), respectively. The symmetrical plane A–A' in Fig. 4(a) behaves as an electric wall or a magnetic wall under the odd-mode or the even-mode excitation, respectively. $Y_{\mathrm{in-odd}}$ and $Y_{\mathrm{in-even}}$ represent the input admittances of the odd-mode and the even-mode equivalent circuits, respectively. The resonant conditions can be derived as

$$Y_{\text{in-odd}} = \frac{Y_0}{j\tan\theta_1} = 0 \tag{1}$$

$$Y_{\text{in-even}} = jY_0\tan(\theta_1+\theta_2) = 0 \tag{2}$$

where θ_1, θ_2, and Y_0 represent electrical lengths and characteristic admittance. The first two resonant frequencies can be accordingly deduced as [21]

$$L_{m1} = \frac{c}{4f_{\text{odd}}\sqrt{\varepsilon_{re}}}, \qquad \text{at } \theta_1 = \pi/2 \tag{3}$$

$$L_{m2} = \frac{c}{2f_{\text{even}}\sqrt{\varepsilon_{re}}} - L_{m1}, \qquad \text{at } \theta_1+\theta_2 = \pi \tag{4}$$

where L_{m1} and L_{m2} are the physical lengths of transmission lines, respectively, and c and ε_{re} are the light speed in free space and the effective dielectric constant, respectively. The conditions for transmission zeros can be derived by

$$\frac{1}{Y_{\text{in}}} = \frac{1-\tan^2\theta_1-2\tan\theta_1\tan\theta_2}{\mathrm{j}2Y_0(\tan\theta_1+\tan\theta_2)} = 0. \tag{5}$$

It can be simplified as

$$2\tan\theta_1\left(\frac{1}{\tan 2\theta_1}-\tan\theta_2\right) = 0 \qquad \tan\theta_1+\tan\theta_2 \neq 0. \tag{6}$$

TABLE I
MAIN DESIGN PARAMETERS OF TSD

Passbands	f_{odd} (GHz)	f_{even} (GHz)	L_{m1} (mm)	L_{m2} (mm)
First	2.97	3.03	17.28	16.6
Second	3.96	4.04	12.96	12.46
Third	4.95	5.05	10.37	9.96

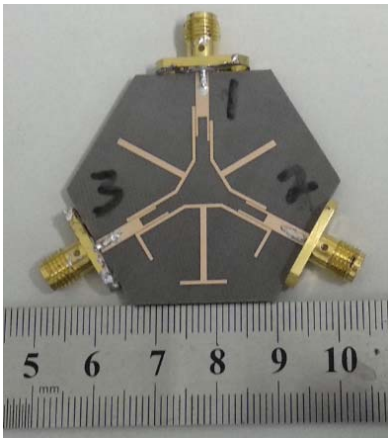

Fig. 5. Photograph of the fabricated TSD.

The condition for the transmission zero near the two modes can be obtained as

$$\tan 2\theta_1 \tan \theta_2 = 1. \tag{7}$$

Thus, the transmission zero near the two modes may appear in the following two cases.

Case 1: According to (3) and (4), if $f_{odd} < f_{even}$, then $\theta_1 > \theta_2$, in this case, (7) illustrates that the condition for a transmission zero near two modes occurrence is $\theta_{1(TZ)} > \pi/2$, and $\theta_{2(TZ)} < \pi/2$. Thus, the transmission zero is allocated on the high side of the two modes when $f_{odd} < f_{even}$.

Case 2: According to (3) and (4), if $f_{odd} > f_{even}$, then $\theta_1 < \theta_2$, in this case, (7) illustrates that the condition for a transmission zero near two modes occurrence is $\theta_{1(TZ)} < \pi/2$, and $\theta_{2(TZ)} > \pi/2$. Thus, the transmission zero is allocated on the low side of the two modes when $f_{odd} > f_{even}$. The reason for the high-frequency selectivity of the TSD is due to the transmission zero located near the two modes.

C. TSD Design and Results

The TSD is designed with the following specifications: the center frequencies of three passbands are set as 3 GHz (f_{TSD1}), 4 GHz (f_{TSD2}), and 5 GHz (f_{TSD3}). As fractional bandwidths of $\Delta 1 = 5\%$, $\Delta 2 = 5\%$, and $\Delta 3 = 5\%$ are chosen, according to (3) and (4), the physical lengths of each SLR can be calculated by the six resonant frequencies of three bands. The main design parameters of the TSD are shown in Table I, and the optimized parameters in Fig. 3 are $W_1 = 0.3$, $W_2 = 2.2$, $W_3 = 0.4$, $W_4 = 1$, $S_1 = 0.15$, $L_1 = 17$, $L_2 = 16.6$, $L_3 = 12.8$, $L_4 = 12.5$, $L_5 = 9.8$, $L_6 = 9.7$, $L_7 = 6.5$, $L_8 = 5.2$, and $L_9 = 4.3$ (unit: mm).

The photograph of the fabricated TSD is depicted in Fig. 5. The overall size of this TSD is about 27.7 mm × 30.3 mm,

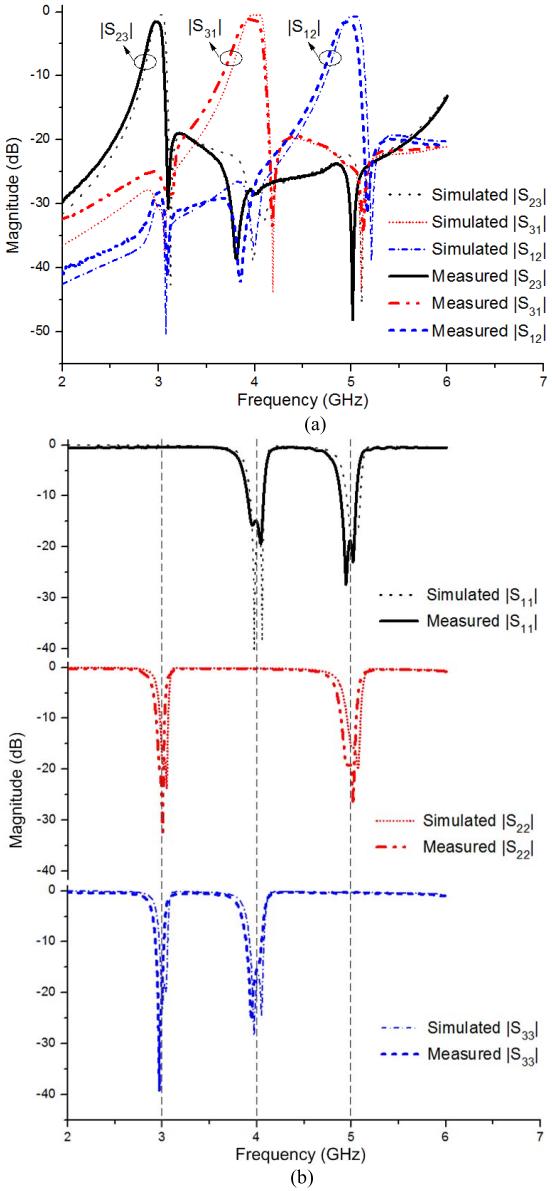

Fig. 6. Simulated and measured results of the designed TSD. (a) Transmission coefficient. (b) Reflection coefficient.

which corresponds to a size of $0.404\lambda_g \times 0.442\lambda_g$, where λ_g is the guided wavelength on the substrate at the center frequency of the first passband. Fig. 6(a) and (b) shows the simulated and measured results. The passband between port 2 and port 3 is designed at 3 GHz (f_{TSD1}), namely, Channel 1, while the passband between port 1 and port 3 is designed at 4 GHz (f_{TSD2}), namely, Channel 2. Finally, the passband between port 1 and port 2 is designed at 5 GHz (f_{TSD3}), namely, Channel 3. The measured results are found in good agreement with the simulated results. In particular, the measured insertion loss is less than 1.5, 1.1, and 1.5 dB at 3, 4, and 5 GHz, respectively. The isolation between different filtering channels is better than 20 dB. Since all of the passbands take the first case, $f_{odd} < f_{even}$, there are three transmission zeros appear on the high side of the three passbands, respectively. The rest of the transmission zeros are generated at other passbands locations, which provide the good channel-to-channel isolation.

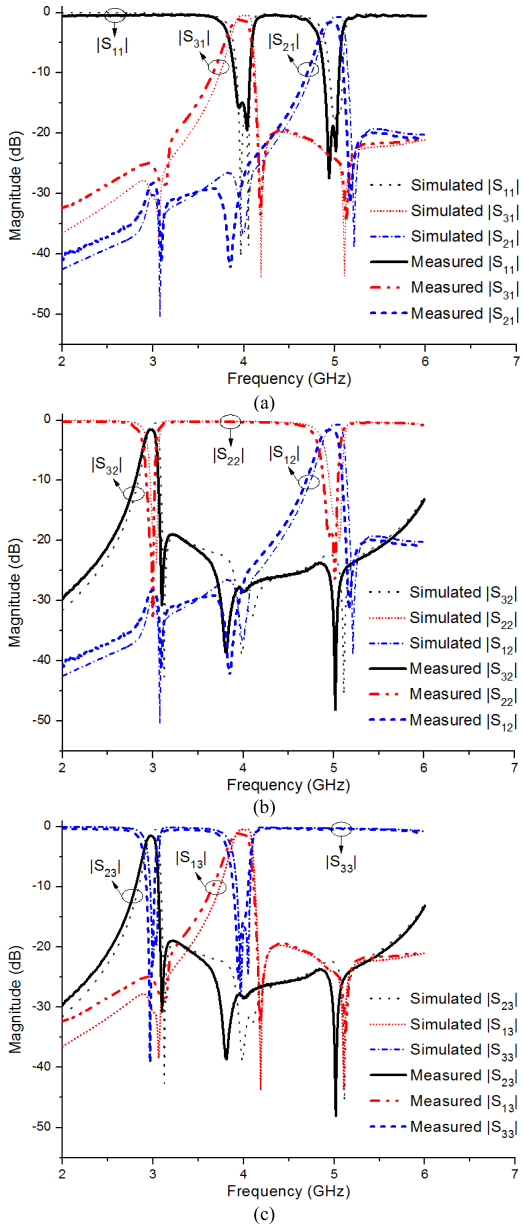

Fig. 7. Simulated and measured results of the designed TSD. (a) Port 1 as the common port. (b) Port 2 as the common port. (c) Port 3 as the common port.

The three states operational functions can be summarized as follows.

State 1: When port 1 is the common port of the diplexer, Channel 2 and Channel 3 can be used as two filtering channels, as shown in Fig. 7(a).

State 2: When port 2 is the common port of the diplexer, Channel 1 and Channel 3 can be used as two filtering channels, as shown in Fig. 7(b).

State 3: When port 3 is the common port of the diplexer, Channel 1 and Channel 2 can be used as two filtering channels, as shown in Fig. 7(c).

III. Second-Order FSD Design

A. Configuration

The corresponding configuration of second-order FSD on the microstrip line structure is shown in Fig. 8. It consists

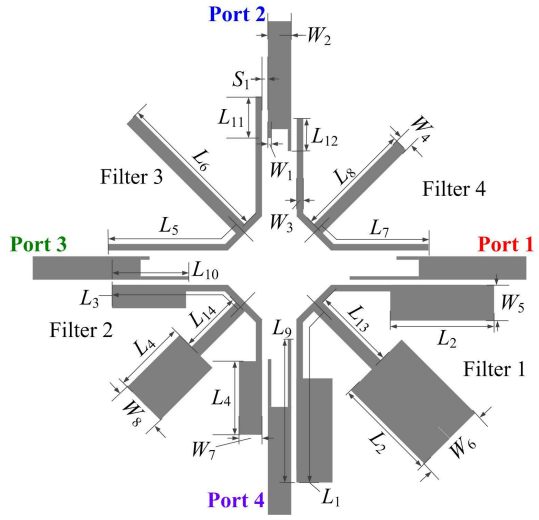

Fig. 8. Configuration of the proposed FSD on the microstrip line structure.

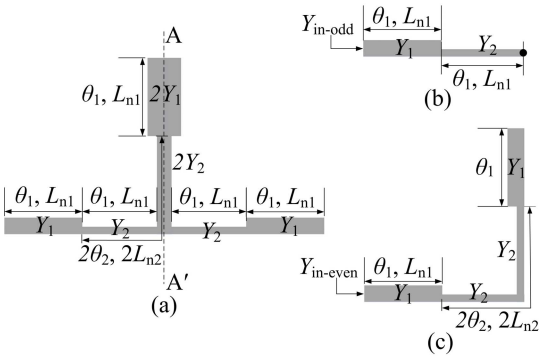

Fig. 9. (a) Layout of SISLR. (b) Odd-mode equivalent circuit. (c) Even-mode equivalent circuit.

of four second-order BPFs and four microstrip feed lines. It involves a uniform-impedance SLR or stepped-impedance SLR (SISLR) [22] in the design of four second-order BPFs. The center frequencies of the four filters (Filter 1, Filter 2, Filter 3, and Filter 4) are denoted by f_{FSD1}, f_{FSD2}, f_{FSD3}, and f_{FSD4}, respectively, wherein $f_{\mathrm{FSD1}} < f_{\mathrm{FSD2}} < f_{\mathrm{FSD3}} < f_{\mathrm{FSD4}}$. Similar to TSD, each state of FSD can also operate at two frequencies but with four operation states in total.

B. Stepped-Impedance Stub-Loaded Resonator

Fig. 9(a) shows the layout of SISLR. The equivalent circuits of odd mode and even mode are depicted in Fig. 9(b) and (c), respectively. $Y_{\mathrm{in-odd}}$ and $Y_{\mathrm{in-even}}$ represent the input admittances of the odd-mode and the even-mode equivalent circuits, respectively. Based on $Y_{\mathrm{in-odd}} = 0$ and $Y_{\mathrm{in-even}} = 0$, the resonant conditions for odd mode and even mode can be derived as [23]

$$\tan^2\theta_1 = Y_2/Y_1, \quad \text{at } f = f_{\mathrm{odd}} \tag{8}$$

$$\tan\theta_1 \tan\theta_2 = Y_2/Y_1, \quad \text{at } f = f_{\mathrm{even}} \tag{9}$$

where θ_1, θ_2 and Y_1, Y_2 represent electrical lengths and characteristic admittances. The first-harmonic resonance of

TABLE II
MAIN DESIGN PARAMETERS OF FSD

Passbands	f_{odd} (GHz)	f_{even} (GHz)	L_{n1} (mm)	L_{n2} (mm)	Y_1 (S)	Y_2 (S)
First	2.03	1.97	8.28	8.79	0.025	0.008
Second	3.03	2.97	5.85	6.09	0.022	0.008
Third	4.06	3.94	6.32	6.7	0.008	0.008
Fourth	5.05	4.95	5.08	5.28	0.008	0.008

odd mode occurs at $f_{\text{s1-odd}}$, and the resonant condition at $f_{\text{s1-odd}}$ can be thus derived as [24]

$$\tan\theta_1 = \infty, \qquad \text{at } f = f_{\text{s1-odd}}. \tag{10}$$

The frequency ratio of odd mode can be deduced as

$$\frac{f_{s1-\text{odd}}}{f_{\text{odd}}} = \frac{\pi}{2\arctan\sqrt{Y_2/Y_1}}. \tag{11}$$

The first-harmonic resonance of even mode occurs at $f_{\text{s1-even}}$. Since the FSD is designed in narrowband with $f_{\text{odd}} \approx f_{\text{even}}$ and $\theta_1 \approx \theta_2$. The resonant condition at $f_{\text{s1-even}}$ can be thus derived as [25]

$$\tan\theta_1 \approx \tan\theta_2 = \infty, \qquad \text{at } f = f_{\text{s1-even}}. \tag{12}$$

Thus, the frequency ratio of even mode can be approximately deduced as

$$\frac{f_{s1-\text{even}}}{f_{\text{even}}} \approx \frac{\pi}{2\arctan\sqrt{Y_2/Y_1}}. \tag{13}$$

Based on the above-mentioned analysis, the resonant frequencies for odd mode and even mode as well as their first harmonic resonant frequencies of each filter can be determined.

C. FSD Design and Results

The FSD is designed with the following specifications: the center frequencies of four passbands are set as 2 GHz (f_{FSD1}), 3 GHz (f_{FSD2}), 4 GHz (f_{FSD3}), and 5 GHz (f_{FSD4}), and the fractional bandwidths $\Delta 1 = 5\%$, $\Delta 2 = 4\%$, $\Delta 3 = 6\%$, and $\Delta 4 = 4\%$ are selected for four bands. Moreover, according to (11) and (13), if $f_{\text{s1}} \approx f_{\text{s1-odd}} \approx f_{\text{s1-even}}$ is suitable for four bands, the frequency ratio $f_{\text{s1(1)}}/f_{\text{o(1)}} = 3.05$, $f_{\text{s1(2)}}/f_{\text{o(2)}} = 2.89$, $f_{\text{s1(3)}}/f_{\text{o(3)}} = 2$, $f_{\text{s1(4)}}/f_{\text{o(4)}} = 2$ are selected. According to (3) and (4), the physical lengths of each SLR can be calculated by the eight resonant frequencies of four bands. The physical lengths of L_{n1} and L_{n2} can be derived as

$$\theta_{1(f_{\text{odd}})} = \arctan\sqrt{Y_2/Y_1} \tag{14}$$

$$L_{n1} = \frac{c\theta_{1(f_{\text{odd}})}}{2\pi f_{\text{odd}}\sqrt{\varepsilon_{re}}} \tag{15}$$

$$\theta_{1(f_{\text{even}})} = \frac{f_{\text{even}}}{f_{\text{odd}}}\theta_{1(f_{\text{odd}})} \tag{16}$$

$$\theta_{2(f_{\text{even}})} = \arctan\sqrt{\frac{Y_2}{Y_1\tan\theta_{1(f_{\text{even}})}}} \tag{17}$$

$$L_{n2} = \frac{c\theta_{2(f_{\text{even}})}}{2\pi f_{\text{even}}\sqrt{\varepsilon_{re}}}. \tag{18}$$

The main design parameters of FSD are shown in Table II, and the optimized parameters in Fig. 7 are $W_1 = 0.3$, $W_2 = 2.2$, $W_3 = 0.4$, $W_4 = 1$, $W_5 = 3$, $W_6 = 6$, $W_7 = 2.5$, $W_8 = 5$, $S_1 = 0.15$, $L_1 = 17$, $L_2 = 8.5$, $L_3 = 12$, $L_4 = 6$, $L_5 = 12.2$, $L_6 = 14.2$, $L_7 = 9.8$, $L_8 = 10.8$, $L_9 = 13.4$, $L_{10} = 7.3$, $L_{11} = 5.3$, $L_{12} = 3.7$, $L_{13} = 7.6$, and $L_{14} = 5.5$ (unit: mm).

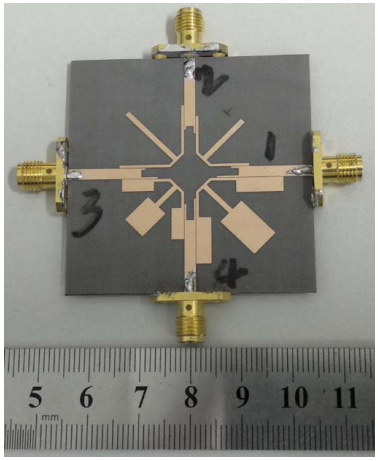

Fig. 10. Photograph of the fabricated FSD.

The photograph of the fabricated FSD is depicted in Fig. 10. The overall size of this FSD is about 32.8 mm × 33.4 mm, which corresponds to $0.319\lambda_{\text{g}} \times 0.325\lambda_{\text{g}}$. Fig. 11(a)–(c) shows the simulated and measured results. The passband between port 1 and port 4 is designed at 2 GHz (f_{FSD1}), namely, Channel 1. The passband between port 4 and port 3 is designed at 3 GHz (f_{FSD2}), namely, Channel 2, while the passband between port 3 and port 2 is designed at 4 GHz (f_{FSD3}), namely, Channel 3. Finally, the passband between port 2 and port 1 is designed at 5 GHz (f_{TSD4}), namely, Channel 4. The measured results agree well with the simulated results. For all of the passbands take the second case, $f_{\text{odd}} > f_{\text{even}}$, each channel has a transmission zero near the lower side of each passband. With the help of these transmission zeros, the selectivity of each passband is improved. The measured insertion loss is less than 1.1, 1.5, 1.2, and 1.6 dB at 2, 3, 4, and 5 GHz, respectively. The isolation between adjacent filtering channels is better than 20 dB. In addition, Fig. 11(c) illustrates the isolation between nonadjacent filtering channels is also better than 20 dB. Finally, It can be observed that the first spurious of the first passband $f_{\text{s1(1)}}$ appears at 6.3 GHz, and the first spurious of the second passband $f_{\text{s1(2)}}$ appears at 8.8 GHz. The results are consistent with theoretical analysis.

The four states operational functions can be summarized as follows.

State 1: When port 1 is the common port of the diplexer, Channel 1 and Channel 4 can be used as two filtering channels, as shown in Fig. 12(a).

State 2: When port 2 is the common port of the diplexer, Channel 4 and Channel 3 can be used as two filtering channels, as shown in Fig. 12(b).

State 3: When port 3 is the common port of the diplexer, Channel 3 and Channel 2 can be used as two filtering channels, as shown in Fig. 12(c).

State 4: When the port 4 is the common port of the diplexer, the Channel 2 and Channel 1 can be used as two filtering channels, as shown in Fig. 12(d).

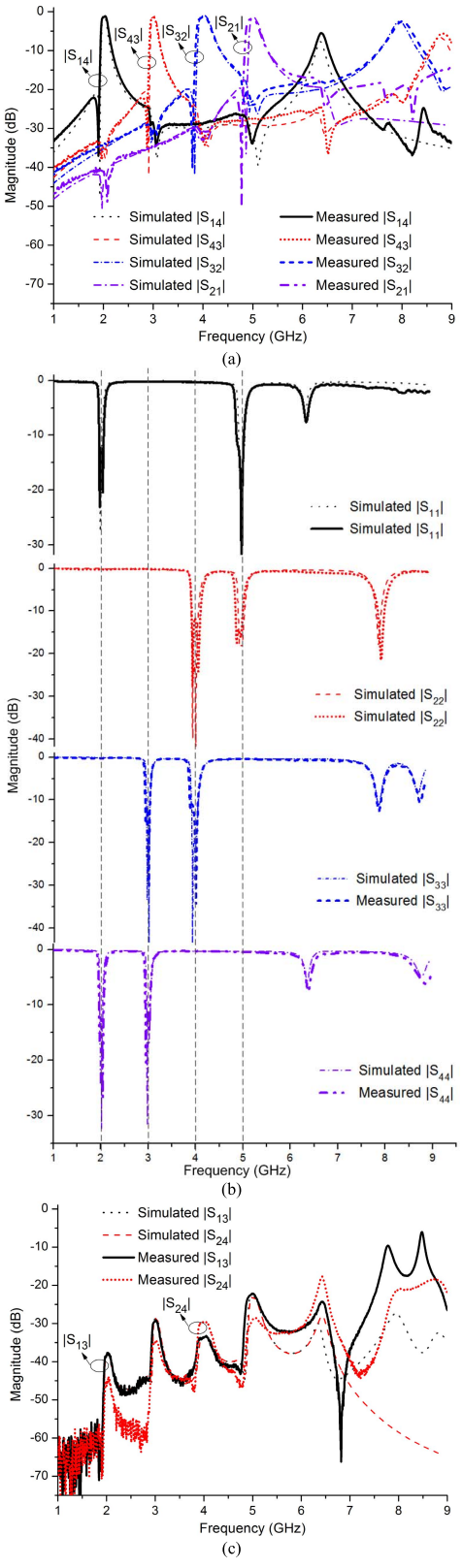

Fig. 11. Simulated and measured results of the designed FSD. (a) Transmisison coefficient. (b) Reflection coefficient. (c) Isolation.

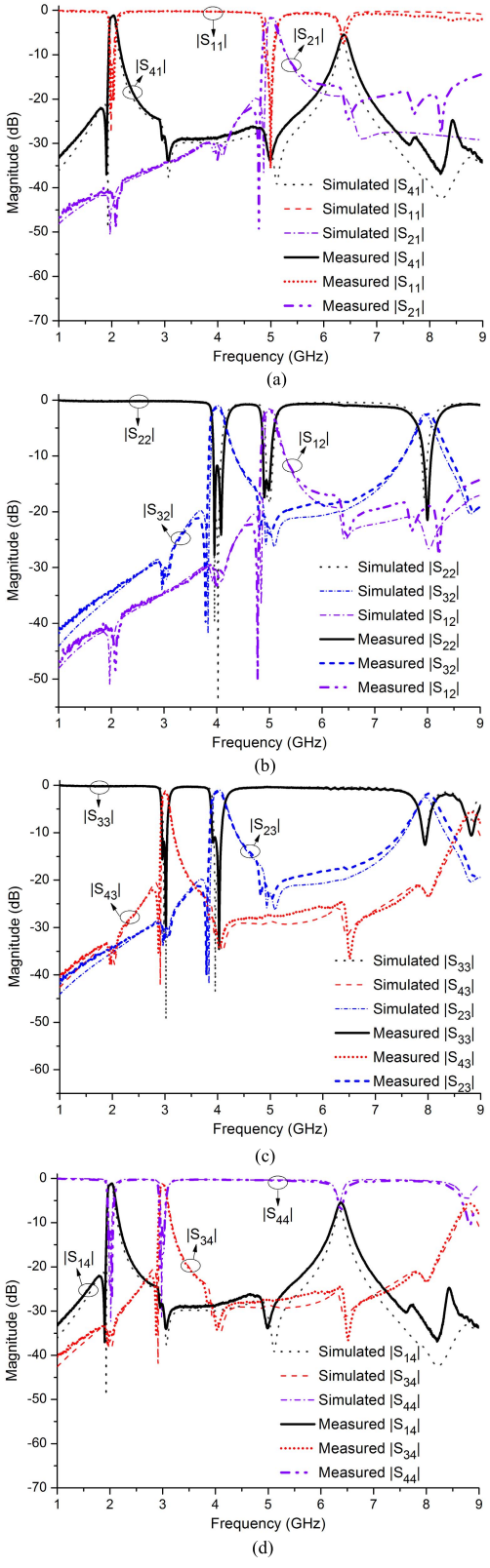

Fig. 12. FSD. (a) Port 1 as the common port. (b) Port 2 as the common port. (c) Port 3 as the common port. (d) Port 4 as the common port.

Table III lists the comparison of the proposed TSD and FSD with other reported TSD, where it is shown that the merits of this paper about small size, low cost, sharp out-of-band rejection skirts, and good isolation.

IV. *m*TH-ORDER *n*-STATE DIPLEXER

Based on the above-described design examples, i.e., TSD and FSD, a generalized *m*th-order *n*-state diplexer can be formed as depicted in Fig. 13. It consists of *n* numbers of

TABLE III
COMPARISONS WITH OTHER REPORTED TSD AND FSD

Ref.	No. of Modes /type of resonator	Circuit Size λ×λ(×λ)	TZs near Each Band	Isolation (dB)	Insertion Loss (dB)
[17]	1/planar	0.48×0.52	No	12	1.5/-/-
[18]	3/cavity	1.2×1.3×1.4	No	27	0.7/0.9/1.4
TSD of this work	2/planar	0.28×0.3	1	20	1.5/1.1/1.5
FSD of this work	2/planar	0.22×0.22	1	20	1.1/1.5/1.2/1.6

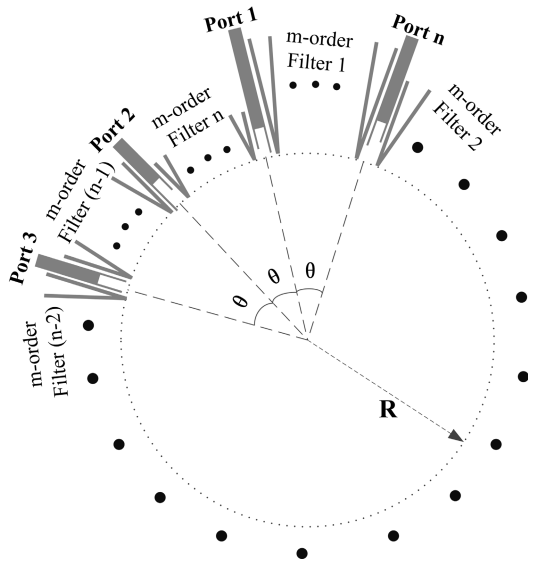

Fig. 13. Configuration of the mth-order n-state diplexer.

mth-order BPFs and n numbers of microstrip feed lines. Each mth-order filter is composed of m resonators with the resonant frequencies at those desired passbands. Without considering the influence of harmonics, this configuration can be extended to achieve an arbitrary number of operation states and arbitrary number of filtering orders in condition of sufficient circuit size. As shown in Fig. 13, with the increase of n and m, θ decreases while R increases. Where θ and R represent the angular radian between adjacent ports and the radius of position circle ($\theta = 2\pi/n$).

V. CONCLUSION

In this paper, the TSD and FSD are presented and designed as the examples of multifunctional diplexers. They are used to achieve a dynamic access of the spectrum and greatly improve the efficiency of spectrum utilization. In this paper, the SLR and SISLR have been applied to build up compact second-order TSD and FSD. Based on the analysis, the TSD and FSD have designed and fabricated. The measured results are found in good agreement with their respective simulated ones, exhibiting low insertion loss, good return loss, sharp out-of-band rejection skirts, and good isolation.

REFERENCES

[1] C.-F. Chen, T.-Y. Huang, C.-P. Chou, and R.-B. Wu, "Microstrip diplexers design with common resonator sections for compact size, but high isolation," *IEEE Trans. Microw. Theory Techn.*, vol. 54, no. 5, pp. 1945–1952, May 2006.

[2] T. Yang, P.-L. Chi, and T. Itoh, "Compact quarter-wave resonator and its applications to miniaturized diplexer and triplexer," *IEEE Trans. Microw. Theory Techn.*, vol. 59, no. 2, pp. 260–269, Feb. 2011.

[3] M.-L. Chuang and M.-T. Wu, "Microstrip diplexer design using common T-shaped resonator," *IEEE Microw. Wireless Compon. Lett.*, vol. 21, no. 11, pp. 583–585, Nov. 2011.

[4] W.-H. Tu and W.-C. Hung, "Microstrip eight-channel diplexer with wide stopband," *IEEE Microw. Wireless Compon. Lett.*, vol. 24, no. 11, pp. 742–744, Nov. 2014.

[5] F.-C. Chen *et al.*, "Design of wide-stopband bandpass filter and diplexer using uniform impedance resonators," *IEEE Trans. Microw. Theory Techn.*, vol. 64, no. 12, pp. 4192–4203, Dec. 2016.

[6] H. J. Tang, W. Hong, J.-X. Chen, G. Q. Luo, and K. Wu, "Development of millimeter-wave planar diplexers based on complementary characters of dual-mode substrate integrated waveguide filters with circular and elliptic cavities," *IEEE Trans. Microw. Theory Techn.*, vol. 55, no. 4, pp. 776–782, Apr. 2007.

[7] Y. Dong and T. Itoh, "Substrate integrated waveguide loaded by complementary split-ring resonators for miniaturized diplexer design," *IEEE Microw. Wireless Compon. Lett.*, vol. 21, no. 1, pp. 10–12, Jan. 2011.

[8] S. Y. Zheng, Z. L. Su, Y. M. Pan, Z. Qamar, and D. Ho, "New dual-/tri-band bandpass filters and diplexer with large frequency ratio," *IEEE Trans. Microw. Theory Techn.*, vol. 66, no. 6, pp. 2978–2992, Jun. 2018.

[9] T. Zheng *et al.*, "Compact superconducting diplexer design with conductor-backed coplanar waveguide structures," *IEEE Trans. Appl. Supercond.*, vol. 25, no. 2, Apr. 2015, Art. no. 1501304.

[10] H. Liu, W. Xu, Z. Zhang, and X. Guan, "Compact diplexer using slotline stepped impedance resonator," *IEEE Microw. Wireless Compon. Lett.*, vol. 23, no. 2, pp. 75–77, Feb. 2013.

[11] A. A. Kirilenko, S. L. Senkevich, V. I. Tkachenko, and B. G. Tysik, "Waveguide diplexer and multiplexer design," *IEEE Trans. Microw. Theory Techn.*, vol. 42, no. 7, pp. 1393–1396, Jul. 1994.

[12] L. Zhu, R. R. Mansour, and M. Yu, "A compact waveguide diplexer employing dual-band resonators," in *IEEE MTT-S Int. Microw. Symp. Dig.*, Jun. 2014, pp. 1–4.

[13] L. Zhu, R. R. Mansour, and M. Yu, "Compact waveguide dual-band filters and diplexers," *IEEE Trans. Microw. Theory Techn.*, vol. 65, no. 5, pp. 1525–1533, May 2017.

[14] K.-L. Wu and W. Meng, "A direct synthesis approach for microwave filters with a complex load and its application to direct diplexer design," *IEEE Trans. Microw. Theory Techn.*, vol. 55, no. 5, pp. 1010–1017, May 2007.

[15] S.-W. Wong, Z.-C. Zhang, S.-F. Feng, F.-C. Chen, L. Zhu, and Q.-X. Chu, "Triple-mode dielectric resonator diplexer for base-station applications," *IEEE Trans. Microw. Theory Techn.*, vol. 63, no. 12, pp. 3947–3953, Dec. 2015.

[16] D. R. Hendry and A. M. Abbosh, "Compact high-isolation base-station duplexer using triple-mode ceramic cavities," *IEEE Trans. Ind. Electron.*, vol. 65, no. 10, pp. 8092–8100, Oct. 2018.

[17] S.-W. Wong *et al.*, "Design of three-state diplexer using a planar triple-mode resonator," *IEEE Trans. Microw. Theory Techn.*, vol. 66, no. 9, pp. 4040–4046, Sep. 2018.

[18] J.-Y. Lin, S.-W. Wong, Y.-M. Wu, L. Zhu, Y. Yang, and Y. He, "A new concept and approach for integration of three-state cavity diplexer based on triple-mode resonators," *IEEE Trans. Microw. Theory Techn.*, vol. 66, no. 12, pp. 5272–5279, Dec. 2018.

[19] J.-S. G. Hong and M. J. Lancaster, *Microstrip Filters for RF / Microwave Applications*. New York, NY, USA: Wiley, 2001.

[20] J. S. Hong, H. Shaman, and Y. H. Chun, "Dual-mode microstrip open-loop resonators and filters," *IEEE Trans. Microw. Theory Techn.*, vol. 55, no. 8, pp. 1764–1770, Aug. 2007.

[21] X. Y. Zhang, J.-X. Chen, Q. Xue, and S.-M. Li, "Dual-band bandpass filters using stub-loaded resonators," *IEEE Microw. Wireless Compon. Lett.*, vol. 17, no. 8, pp. 583–585, Aug. 2007.

[22] Z.-C. Zhang, Q.-X. Chu, and F.-C. Chen, "Novel quad-band filter with high frequency ratio and controllable bandwidths using SLHSIRs and SLQSIRs," *Microw. Opt. Technol. Lett.*, vol. 56, no. 12, pp. 2845–2848, Dec. 2014.

[23] Q.-X. Chu and X.-K. Tian, "Design of UWB bandpass filter using stepped-impedance stub-loaded resonator," *IEEE Microw. Wireless Compon. Lett.*, vol. 20, no. 9, pp. 501–503, Sep. 2010.

[24] Q.-X. Chu and F.-C. Chen, "A compact dual-band bandpass filter using meandering stepped impedance resonators," *IEEE Microw. Wireless Compon. Lett.*, vol. 18, no. 5, pp. 320–322, May 2008.
[25] S. Sun and L. Zhu, "Compact dual-band microstrip bandpass filter without external feeds," *IEEE Microw. Wireless Compon. Lett.*, vol. 15, no. 10, pp. 644–646, Oct. 2005.

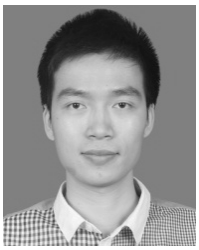

Zhi-Chong Zhang was born in Ji'an, Jiangxi, China, in 1988. He received the B.S. degree in communication engineering from Nanchang University, Nanchang, China, in 2008, the M.E. degree in communication and information system from the East China Jiaotong University, Nanchang, in 2012, and the Ph.D. degree in electromagnetic fields and microwave technology from the South China University of Technology, Guangzhou, China, in 2015.

Since 2016, he has been a Lecturer with the School of Electronic and Information Engineering, Jinggangshan University, Ji'an. His current research interests include the design of microwave filters and associated RF modules for microwave and millimeter-wave applications.

Sai-Wai Wong (S'06–M'09–SM'14) received the B.S degree in electronic engineering from the Hong Kong University of Science and Technology, Hong Kong, in 2003, and the M.Sc. and Ph.D. degrees in communication engineering from Nanyang Technological University, Singapore, in 2006 and 2009, respectively.

From 2003 to 2005, he was the lead of the Engineering Department in the mainland of China with two Hong Kong manufacturing companies. From 2009 to 2010, he was a Research Fellow with the Institute for Infocomm Research, Singapore. Since 2010, he has been an Associate Professor and a Full Professor with the School of Electronic and Information Engineering, South China University of Technology, Guangzhou, China. In 2016, he joined the City University of Hong Kong, Hong Kong, as a Visiting Professor. Since 2017, he has been a Full Professor with the College of Information, Shenzhen University, Shenzhen, China. His current research interests include RF/microwave circuit and antenna design.

Dr. Wong was a recipient of the New Century Excellent Talents in University Award in 2013 and the Shenzhen Overseas High-Caliber Personnel Level C in 2018. He is a Reviewer for several top-tier journals.

Jing-Yu Lin (S'14) received the B.E. degree from Southwest Jiaotong University, Chengdu, China, in 2016, and the M.E. degree from the School of Electronic and Information Engineering, South China University of Technology, Guangzhou, China, in 2018. He is currently pursuing the Ph.D. degree at the University of Technology Sydney, Ultimo, NSW, Australia.

His current research interests include microwave cavity circuit design.

Haiwen Liu (M'04–SM'13) received the B.S. degree in electronic system and the M.S. degree in radio physics from Wuhan University, Wuhan, China, in 1997 and 2000, respectively, and the Ph.D. degree in microwave engineering from Shanghai Jiao Tong University, Shanghai, China, in 2004.

From 2004 to 2006, he was a Research Assistant Professor with Waseda University, Tokyo, Japan. From 2006 to 2007, he was a Research Fellow with Kiel University, Kiel, Germany, granted by the Alexander von Humboldt Research Fellowship. From 2007 to 2008, he was a Professor with the Institute of Optics and Electronics, Chengdu, China, supported by the 100 Talents Program of Chinese Academy of Sciences. From 2009 to 2017, he was a Chair Professor with East China Jiaotong University, Nanchang, China. In 2014, he joined Duke University, Durham, NC, USA, as a Visiting Scholar. In 2015, he joined the University of Tokyo, Tokyo, as a Visiting Professor, supported by the JSPS Invitation Fellowship. In 2016, he joined the City University of Hong Kong, Hong Kong, as a Visiting Professor. Since 2017, he has been a Full-Time Professor with Xi'an Jiaotong University, Xi'an, China. He has authored or co-authored more than 100 papers in international and domestic journals and conferences. His current research interests include electromagnetic modeling of high-temperature superconducting circuits, RF and microwave passive circuits and systems, synthesis theory and practices of microwave filters and devices, antennas for wireless terminals, and radar system.

Dr. Liu has served as the Editor-in-Chief of the *International Journal of RF and Microwave Computer-Aided Engineering* (Wiley), an Associate Editor of IEEE ACCESS, and the Guest Chief Editor of the *International Journal of Antennas and Propagation*. He was the Executive Chairman of the National Antenna Conference of China in 2015 and the Co-Chairman of the National Compressive Sensing Workshop of China in 2011 and the Communication Development Workshop of China in 2016.

Lei Zhu (S'91–M'93–SM'00–F'12) received the B.Eng. and M.Eng. degrees in radio engineering from the Nanjing Institute of Technology (now Southeast University), Nanjing, China, in 1985 and 1988, respectively, and the Ph.D. degree in electronic engineering from the University of Electro-Communications, Tokyo, Japan, in 1993.

From 1993 to 1996, he was a Research Engineer with Matsushita–Kotobuki Electronics Industries Ltd., Tokyo. From 1996 to 2000, he was a Research Fellow with the École Polytechnique de Montreal, Montreal, QC, Canada. From 2000 to 2013, he was an Associate Professor with the School of Electrical and Electronic Engineering, Nanyang Technological University, Singapore. In 2013, he joined the Faculty of Science and Technology, University of Macau, Macau, China, as a Full Professor and has been a Distinguished Professor since 2016. From 2014 to 2017, he served as the Head of the Department of Electrical and Computer Engineering, University of Macau. He has authored or co-authored more than 420 papers in international journals and conference proceedings. His papers have been cited more than 5250 times with an H-index of 39 (source: ISI Web of Science). His current research interests include microwave circuits, guided-wave periodic structures, planar antennas, and computational electromagnetic techniques.

Dr. Zhu served as a member for the IEEE MTT-S Fellow Evaluation Committee from 2013 to 2015 and the IEEE AP-S Fellows Committee from 2015 to 2017. He was a recipient of the 1997 Asia–Pacific Microwave Prize Award, the 1996 Silver Award of Excellent Invention from Matsushita-Kotobuki Electronics Industries Ltd., and the 1993 First-Order Achievement Award in Science and Technology from the National Education Committee, China. He was the Associate Editor of the IEEE TRANSACTIONS ON MICROWAVE THEORY AND TECHNIQUES from 2010 to 2013 and IEEE MICROWAVE AND WIRELESS COMPONENTS LETTERS from 2006 to 2012. He served as the General Chair for the 2008 IEEE MTT-S International Microwave Workshop Series on the Art of Miniaturizing RF and Microwave Passive Components, Chengdu, China, and the Technical Program Committee Co-Chair of the 2009 Asia–Pacific Microwave Conference, Singapore.

Yejun He (SM'09) received the Ph.D. degree in information and communication engineering from the Huazhong University of Science and Technology, Wuhan, China, in 2005.

From 2005 to 2006, he was a Research Associate with the Department of Electronic and Information Engineering, The Hong Kong Polytechnic University, Hong Kong. From 2006 to 2007, he was a Research Associate with the Department of Electronic Engineering, Faculty of Engineering, The Chinese University of Hong Kong, Hong Kong. In 2012, he joined the Department of Electrical and Computer Engineering, University of Waterloo, Waterloo, ON, Canada, as a Visiting Professor. From 2013 to 2015, he was an Advanced Visiting Scholar (Visiting Professor) with the School of Electrical and Computer Engineering, Georgia Institute of Technology, Atlanta, GA, USA. Since 2011, he has been a Full Professor with the College of Information Engineering, Shenzhen University, Shenzhen, China, where he is currently the Director of the Guangdong Engineering Research Center of Base Station Antennas and Propagation, the Director of the Shenzhen Key Laboratory of Antennas and Propagation, and the Vice Director of the Shenzhen Engineering Research Center of Base Station Antennas and Radio Frequency. He has authored or co-authored over 100 research papers and books (chapters). He holds about 20 patents. His current research interests include wireless mobile communication, antennas, and RF.

Dr. He is a Fellow of the IET. He has also served as a Technical Program Committee member or a Session Chair for various conferences, including the IEEE Global Telecommunications Conference, the IEEE International Conference on Communications, the IEEE Wireless Communication Networking Conference, and the IEEE Vehicular Technology Conference. He has served as a Reviewer for various journals such as the IEEE TRANSACTIONS ON VEHICULAR TECHNOLOGY, the IEEE TRANSACTIONS ON COMMUNICATIONS, the IEEE TRANSACTIONS ON WIRELESS COMMUNICATIONS, the IEEE TRANSACTIONS ON INDUSTRIAL ELECTRONICS, IEEE *Wireless Communications*, IEEE *Communications Letters*, the IEEE JOURNAL ON SELECTED AREAS IN COMMUNICATIONS, the *International Journal of Communication Systems, Wireless Communications and Mobile Computing*, and the *Wireless Personal Communications*. He is currently serving as an Associate Editor for IEEE ACCESS and *Security and Communication Networks*.